



CT and MR perfusion techniques to assess diffuse liver disease

Maxime Ronot^{1,2,3} · Benjamin Leporq^{1,2,3} · Bernard E. Van Beers^{1,2,3} · Valérie Vilgrain^{1,2,3}

Published online: 25 November 2019

© Springer Science+Business Media, LLC, part of Springer Nature 2019

Abstract

Perfusion imaging allows for the quantitative extraction of physiological perfusion parameters of the liver microcirculation at levels far below the spatial resolution of CT and MR imaging. Because of its peculiar structure and architecture, perfusion imaging is more challenging in the liver than in other organs. Indeed, the liver is a mobile organ and significantly deforms with respiratory motion. Moreover, it has a dual vascular supply and the sinusoidal capillaries are fenestrated in the normal liver. Using extracellular contrast agents, perfusion imaging has shown its ability to discriminate patients with various stages of liver fibrosis. The recent introduction of hepatobiliary contrast agents enables quantification of both the liver perfusion and the hepatocyte transport function using advanced perfusion models. The purpose of this review article is to describe the characteristics of liver perfusion imaging to assess chronic liver disease, with a special focus on CT and MR imaging.

Keywords Perfusion imaging · Liver cirrhosis · Fibrosis · Hepatic artery · Microcirculation

Introduction

The liver is a large, richly vascularized, and subcutaneous abdominal organ. Imaging plays a central role in the assessment of both diffuse and focal liver diseases. Many imaging techniques, including computed tomography (CT) and magnetic resonance imaging (MRI), are routinely used. It is important to differentiate conventional imaging analyses, based on the dynamic enhancement of tissues, from perfusion imaging that allows for the quantitative extraction of physiological perfusion parameters of the liver. As such, perfusion imaging provides quantitative information about tissue microcirculation and at levels far below the spatial resolution of these imaging techniques. As in other organs, perfusion imaging relies on the injection of a contrast medium called a tracer and on the acquisition of signal intensity/time curves that monitor the variation in tracer concentrations over time. These curves can either be described or inform dedicated mathematical perfusion models. Because of its

peculiar structure and architecture, perfusion imaging is more challenging in the liver than in other organs. Indeed, the liver is a mobile organ and significantly deforms with respiratory motion. Moreover, it has a dual vascular supply through the hepatic artery and the portal vein. Finally, the sinusoidal capillaries are fenestrated in the normal liver and the tracer easily diffuses from them.

Perfusion imaging has been developed in the liver for the assessment of malignant liver tumors—especially hepatocellular carcinoma and liver metastases—and for the exploration of chronic liver diseases, which will be the topic of the present article. Since cross-sectional imaging plays an important role in the assessment of many chronic liver diseases, perfusion imaging should not replace conventional imaging. It should rather be seen as a possible complementary tool aiming to refine patient management or provide earlier and more reproducible disease evaluation. The purpose of this article is to describe the characteristics of liver perfusion imaging to assess chronic liver disease, with a special focus on CT and MR imaging.

✉ Maxime Ronot
maxime.ronot@aphp.fr

¹ Department of Radiology, APHP, University Hospitals Paris Nord Val de Seine, Beaujon, Clichy, Hauts-de-Seine, France

² University of Paris, Paris, France

³ Laboratory of Imaging Biomarkers, INSERM U1149, Centre for Research on Inflammation, Paris, France

The vascular physiology of the liver

The liver receives a dual blood supply. Approximately, one quarter of its blood supply comes from the hepatic artery, and the remaining is provided by the portal vein.

There is no hepatic capillary network per se as sinusoids are fenestrated. In a normal liver, the two afferent vascular systems freely communicate through trans-sinusoidal, transvasal communications, and through the peribiliary plexuses. The portal perfusion significantly varies over time depending on the splanchnic venous flow (i.e., fasting or post-prandial). It is also influenced by respiratory movements.

In patients with chronic liver diseases, fibrogenesis causes significant changes in hepatic architecture and function. Chronic liver injuries (e.g., viral infection, toxic exposure, or dysregulation in metabolic metabolism) leads to infiltration of the hepatic parenchyma by inflammatory macrophages. They release fibrogenic mediators that activate the hepatic stellate cells. These cells located in the Disse space undergo phenotypical activation into myofibroblasts that eventually secrete large amounts of extracellular matrix proteins. The consequence is the progressive deposition of extravascular fibrosis and sinusoidal capillarization, i.e., loss of sinusoidal fenestrations. The capillarization of the sinusoids, the enlargement of the extravascular space, and the contraction of the activated stellate cells progressively decrease the volume of the sinusoidal space, increase intrahepatic vascular resistance [1, 2], leading to portal venous perfusion decrease. The key adaptive mechanisms of the liver vascular physiology one needs to understand to fully grasp the complexity of liver perfusion is the presence of an arteriportal balance referred to as the ‘hepatic buffer response’. In normal liver, a drop in portal perfusion is, at least partially compensated, by an increase in arterial blood supply [3]. Importantly, the reverse does not occur. In chronic liver diseases, the decrease in portal perfusion is only partly compensated by the buffer response and the resulting global liver perfusion decreases.

Imaging techniques for perfusion imaging

Ideally, liver perfusion analysis should fulfill many requirements [4]:

- Whole liver imaging;
- High spatial resolution to examine;
- High temporal resolution to correctly monitor the kinetics of tracers;
- Ability to provide both overall and regional arterial and portal perfusion;
- Accurate measurement of tracer concentrations;
- Robust and validated modeling of the physiology of liver perfusion;
- Compatibility with conventional imaging techniques (e.g., CT and MR imaging) so that perfusion studies can be easily performed in routine.

Whatever the imaging technique, time-resolved acquisitions are mandatory to accurately and quantitatively monitor tracer kinetics. A compromise between high spatial resolution and extensive coverage is to be found. The later is very important, but decreases the maximum temporal resolution. In practice, the spatial resolution and the volume are reduced to obtain satisfactory temporal resolution. This may be problematic in diffuse diseases with locoregional variations. In this regard, CT and MR imaging offer advantages and drawbacks that radiologists need to be aware of (Table 1).

Computed tomography

The use of CT offers several advantages. It is inexpensive, quick, and accessible. Spatial and temporal resolution are high, and quantification of the tracer concentration is straightforward as changes in attenuation (in Hounsfield units) is proportional to the variation of concentration of the tracer over time. Its limitations are also well known: injection of the iodinated contrast and radiation exposure. Perfusion imaging is responsible for limited additional dose deposition to the patients.

Several acquisition protocols have been reported, with significant variation in terms of duration of acquisition, organ coverage, and time sampling. Whatever the acquisition protocol, the quality of injection is key to obtain reliable perfusion imaging analysis. In our department, the contrast agents (350 mg of iodine/mL) is injected at a rate of 4 mL/s. Since image acquisition lasts for few minutes, respiratory artifacts are present and need to be reduced. To do so, patients are asked to breathe superficially and slowly. They are also told about a possible flush sensation they may experience after the injection.

MR imaging techniques

Dynamic contrast-enhanced MRI

Several MRI approaches have been described to analyze the hepatic microcirculation. The most common approach

Table 1 Advantages and limitations of CT and MR imaging modalities to study liver perfusion

	CT	MR imaging
Spatial resolution	+++	+
Temporal resolution	++	++
Measurement of tracer concentration alone	+++	+
“Whole liver” imaging	+	+++
Modeling	+/-	+/-
Association with morphological imaging	++	+++

+ average, ++ good, +++ excellent, ± problematic

is a kinetic analysis following injection of a bolus of contrast material. The contrast may induce “negative enhancement” (i.e., signal drop due to the effects induced by the first pass of a bolus of concentrated contrast agent in T2/T2*-weighted MRI sequences). The corresponding technique is called dynamic susceptibility contrast MRI (DSC-MRI). Nowadays, it is mostly indicated in brain perfusion analysis. The main reason is that, strictly speaking, DSC-MRI is not used to assess capillary leakage because it assumes the presence of an blood-organ barrier that is impermeable to contrast agents. Since hepatic sinusoids are fenestrated, it is not used in the liver.

The quantification of positive enhancement (the so called ‘T1 effect’ of the contrast agent) is called “dynamic contrast-enhanced-imaging” (DCE imaging). It is by far the most common technique used in the liver. To perform DCE-MR imaging, sequences are accelerated (or time resolved) to obtain multiple dynamic scans [5]. As stated above, high temporal resolution is needed because of the rapid changes in tracer concentration, changes in the arterial vessels during the first pass, and accurate sampling of the concentration versus time curves is essential. A temporal resolution lower than 3 s is therefore recommended, but a resolution of one second may be needed to sample the aortic peak enhancement. To improve the temporal resolution, partial k -space updating methods are increasingly used. These imaging sequences use central k -space filling and keyhole acquisitions. They can be combined with partial Fourier and parallel imaging to further decrease the dynamic acquisition time. It offers the possibility to improve organ coverage (ideally the entire liver), with acceptable spatial and temporal resolution [6–9]. The k -space filling scheme used in these sequences also reduces motion sensitivity which is an important issue for free-breathing perfusion imaging. Nevertheless, it remains difficult to obtain such time resolution for whole liver 3D MRI.

Perfusion imaging is more challenging with MR imaging because the relationship between tracer concentrations and signal intensity are not linear. Perfusion imaging does not require the relationship to be linear (as it is in CT), but must be well known. Several strategies have been described to address this non-linear relationship. First, pre-calibration can be performed by acquiring images with different tracer concentrations [10, 11]. This method is very accurate, but is difficult to perform in routine clinical practice. Autocalibration is a valid alternative. This requires computing a T_1 pre-contrast map with a multiple angle acquisition corresponding to a dynamic acquisition flip angle in order to derive the post-injection T_1 . Finally, tracer concentrations can be determined if its relaxivity (r_1) is known. This is interesting since the relationship between r_1 and the tracer concentration is linear. This method is sensitive to the non-uniformity of the transmitted B_1 field as well as to the non-linearity of

the RF transmission chain which affects small flip angles in particular, especially with 2D acquisitions, but it can be corrected using a B_1 mapping. Moreover, these measurements need be obtained from 3D images because of the imperfect slice selection profile of 2D images. Finally, and pragmatically, a linear relationship between contrast agent concentrations and signal intensity is often assumed. In this case, low contrast agent concentrations (0.025 mmol/kg) and/or lower injection rates are recommended to avoid signal enhancement saturation at high concentrations. The pulse sequence setting should also be carefully performed to minimize the non-linearity effect. While most teams use extracellular gadolinium chelates, recent studies have reported the use of liver-specific contrast agents, reporting similar results [12].

Intravoxel incoherent motion model

Besides DCE-MR imaging, sequences that are sensitive to molecular diffusion (diffusion-weighted MRI) are also influenced by microperfusion. This concept, which is called the intravoxel incoherent motion (IVIM) model, was initially developed by Le Bihan et al. [13] to quantitatively measure the microscopic movements that contribute to the diffusion MR signal. In tissue, these movements are known to be mainly due to the molecular diffusion of water and the microcirculation of blood in the capillary network. Le Bihan et al. have developed the idea that the motion of water molecules circulating in randomly oriented capillaries (at a voxel level) can be approximated as random motion, hence the term “pseudodiffusion”. This results in diffusion signal attenuation and depends upon the vascular architecture and the speed of the circulating blood. Similar to actual molecular diffusion, the influence of pseudodiffusion on signal attenuation heavily depends on the b value. Importantly, the amount of signal attenuation associated with pseudodiffusion is significantly greater than that resulting from molecular diffusion. As a result, the relative contribution of each to the diffusion-weighted signal is only significant at very low b values, allowing diffusion and microperfusion to be separated.

Liver perfusion modeling

As stated above, perfusion imaging relies on the quantitative analysis of tracer concentration–time curves (Fig. 1) whose shape depends on tissue perfusion parameters (Table 2), the characteristics of the tracer bolus (volume and injection rate), and the patient’s cardiovascular parameters (cardiac output and ejection fraction).

Two main mathematical approaches have been described to analyze the hepatic perfusion: a semi-quantitative approach that is based on the analysis of the shape of the

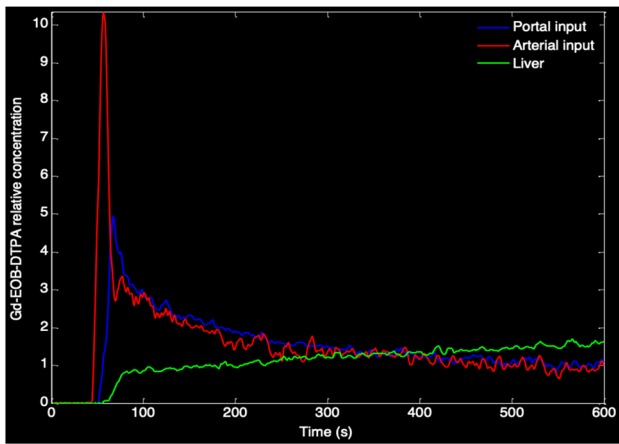


Fig. 1 Example of signal intensity/time curve. The red line shows the aortic peak enhancement. The blue and green ones show the portal vein and liver parenchyma enhancement, respectively

signal intensity/time curves (descriptive methods), and a quantitative approach based on various perfusion model that are informed by the curves (pharmacokinetic approach).

Descriptive methods of attenuation or signal intensity/time curves are free of any physiological hypothesis about the liver microcirculation (free models). The curves are automatically analyzed by dedicated shape recognition software in order to produce perfusion maps. Several descriptive or “heuristic” parameters can be derived from the enhancement curves, such as the slope of enhancement (maximum slope), maximum enhancement (peak height) expressed in a percentage, and the time-to-peak. Descriptive methods are highly sensitive to curves instability caused by liver and vessel displacement. The area under the curve (AUC), i.e., the integral under the enhancement curve, is also a common parameter because it is less affected by noise and does not require a mathematical model [14].

Raw semi-quantitative evaluations do not take into account the intra-arterial kinetics of the tracer that may significantly differ among patients depending on the injection

parameters (iodine concentration, volume of contrast, injection rate, etc.) and physiological conditions (cardiac output, respiration, etc.). The resulting variations of arterial input function may be taken into account by comparing the liver perfusion to that of a reference tissue such as the muscle or a normal area of the liver. Correction is often performed by computing ratios to obtain relative parameters. These simple approaches are very sensitive to the quality of the acquisitions.

Pharmacokinetic models are built on known characteristics of hepatic perfusion. Most of them are based on the relationship between arterial and portal venous input obtained from the signal enhancement curves of the afferent blood vessels. Compartmental models and deconvolution algorithms [15, 16] belong to this category. The latter represents the hepatic microcirculation as a conjunction of compartments in which the tracer concentration is uniform. Flow between compartments is assumed to be linear (i.e., exchanges are only passive) and parameters describing compartments are considered invariable during data acquisition. The different parameters of interest are then extracted by fitting the models. The nature and the number of parameters depends on the model (number of compartments, type of exchange between compartment, role of afferent blood vessels, etc.).

The two vascular inputs of the liver (i.e., arterial and portal) justify the use of dual-input models. A single-compartmental model proposed by Materne and Van Beers [10] is often used. It has been validated with radiolabeled microspheres. This models allows for the quantification of the arterial, portal venous, and total liver blood transfer constants k_{1a} , k_{1p} , and k_{1t} ($\text{mL min}^{-1} 100 \text{ mL}^{-1}$), as well as the hepatic reflux rate k_2 ($\text{mL min}^{-1} 100 \text{ mL}^{-1}$). The perfusion fraction (%) is given by k_{1a}/k_{1t} , the distribution volume (DV: %) by $k_2/(k_{1a} + k_{1p})$, and the mean transit time (MTT: s) by $1/k_2$.

K_1 represents the combination of perfusion and permeability and is given by $K_1 = F \times E$, in which F is the perfusion and E is the extraction fraction (value between 0 and 1).

Table 2 Glossary of perfusion parameters

Parameter	Definition	Unit
Time-to-peak	Time between arrival of the tracer in large afferent vessels and maximum enhancement	Second
Blood flow	Flow rate of the blood per unit of time	mL min^{-1}
Perfusion	Flow rate of the blood per unit of time and per unit of mass or volume of tissue	$\text{mL } 100 \text{ g}^{-1} \text{ min}^{-1}$
Blood volume	Volume of blood flowing blood within vasculature	$\text{mL } 100 \text{ g}^{-1}$
Mean transit time	Average time(s) for blood to traverse from arterial to the venous end of the vasculature.	Second
Permeability	Unidirectional flux rate of contrast agent from the blood plasma into the liver parenchyma (i.e., interstitial space) normalized by the total surface area of capillaries per unit mass of tissue. I	$\text{mL } 100 \text{ g}^{-1} \text{ min}^{-1}$
Arterial/venous perfusion index	Amount of blood entering the region of interest through the arterial/venous network	%

When permeability is high as in the normal liver—because of the fenestrated sinusoids—the extraction fraction is assumed to be equal to one and K_1 represents the perfusion only. If permeability is lower (in patients with chronic liver disease for instance), K_1 represents the permeability-surface area product (PS) [17].

The vascular inputs are measured with a region of interest (ROI) drawn in the abdominal aorta (as surrogate for the hepatic artery) and the portal vein. When dual-input one-compartment models are used, two different delays (arterial and portal venous) need to be implemented in the model to take into consideration the temporal offset between central compartment input and measured input from arterial and portal ROIs [11]. Of course, the addition of two fitting parameters in the model significantly increases the degree of freedom involving multiple local minima problems. Therefore, authors have proposed to set the delays manually. While arterial delay can be easily derived from a curve analysis, manual estimation of portal venous delay is more challenging. To address this, researches have considered the arterial and portal venous delays to be equal [10]. Others have set the portal venous delay to zero [12]. An interesting method is to include both delays in the model and use advanced optimization procedures such as multistart approaches for the fitting procedure [11]. The main limitation of these approaches is the computing time increase due to the repetition of fitting procedure.

Difficulties of perfusion imaging of the liver

Fasting state, liver movement

Studies using fixed landmarks have shown that the liver is an organ that moves considerably during breathing, shifting approximately 20 mm along its head-foot axis, 10 mm along its anteroposterior axis, and 5 mm laterally [18]. Because of long acquisition times (at least 2–3 min), free-breathing is necessary during perfusion imaging acquisitions. To limit pixel scale mismatches so that quantitative data analysis remain accurate, correct registration of the different images/time points is of utmost importance.

In a non-co-registered data set of $2D + t$ images, respiratory motion may introduce temporal noise in both input and tissue functions, thus reducing the robustness of the perfusion modeling. For anatomical reasons, this effect is more problematic with the portal venous input function. Indeed, the orientation of the portal vein with regard to the main axis of displacement (cranio-caudal) creates significant mismatches. To limit this effect, coronal views may be favored over transverse ones. Another possibility is to include a registration-based motion correction method in the post-processing chain.

Several registration-based methods correct respiratory motion and are classified according to the search space used (rigid, elastic, and optical flow). The choice of the best method to correct for respiratory motion artifacts in quantitative perfusion imaging of the liver is still a matter of debate. Assuming that liver displacements induced by respiratory motion do not change the liver volume and morphology, rigid registration-based motion correction by the geometric approach seems to be the most accurate approach [7].

New generation of motion insensitive pulse sequence based on specific k -space sampling such as golden-angle radial sparse parallel (GRASP) may provide significant improvement since it is possible to perform measurements without images registration [19, 20]. This pulse sequence can be coupled with compressed sensing to speed up acquisition (extra-dimensional golden-angle radial sparse parallel imaging, XD-GRASP) and to acquire simultaneous high spatial and temporal resolution [21]. The GRASP technique exploits joint multicoil sparsity techniques to allow continuous acquisition of dynamic information. During image reconstruction, data are sorted into sequential timeframes and then reconstructed using highly undersampled data in a multicoil compressed sensing iterative method [22]. The same dataset can be grouped after acquisition into time frames at any desired temporal reconstruction, to a resolution of as low as 2 s per frame, resulting in highly flexible retrospective analysis that offers higher robustness to the respiratory motion and flow. However, images reconstruction required high computing power and, at this time, the processing time remains important (dependently of desired spatial and temporal resolutions). However, recent MR systems with GPUs parallel computing significantly improve the computation time.

Importantly, liver perfusion measurements should be performed in a fasted state, as the portal venous flow is known to significantly increase after a meal, thus changing the hepatic arterial-portal venous balance [23].

The reproducibility issue

The reproducibility of perfusion imaging depends on acquisition protocols, reconstruction methods, and of course the software used for quantitative analysis [24–26]. Therefore, acquisition protocols should be standardized as much as possible, and multi-center studies with centralized analysis should be favored to improve uniformity [27]. It has also been recommended to assess repeatability before beginning clinical trials including perfusion imaging of the liver. This is especially important when changes of perfusion parameter are used as endpoints (e.g., to assess response to treatment). In this setting, the estimated effect on perfusion (critical % change) should be higher than the repeatability index (%) which corresponds to $2.77 \times wCV \times 100\%$, where wCV is

the within-subject coefficient of variation. Ktrans has an estimated wCV of 15–20% based on publications. As a consequence, a change of approximately 40–55% is needed in a single subject to be considered significant [28].

Application of perfusion imaging in chronic liver disease

Perfusion imaging with extracellular contrast agents

The first studies evaluating chronic liver diseases with perfusion CT were published in the 1990s by Miles et al. and Blomley et al. Authors described the hepatic buffer response using a semi-quantitative slope model [29, 30]. Using the abovementioned dual-input one compartmental model, our team has shown that perfusion imaging was capable of quantifying the decrease of total liver perfusion and the compensatory increase in arterial fraction and mean transit time in patients with cirrhosis compared to controls and patients with advanced fibrosis [31]. We also showed that perfusion CT could discriminate patients with early stages of liver fibrosis. This was counterbalanced by the significant overlap in the measured parameters between fibrosis stages limiting the practical utility of the results [32].

These results have been confirmed in several animal models of chronic liver diseases using DCE-MR imaging [10, 33, 34]. Similar to CT, we and others have described the reduction in portal venous perfusion and the compensatory increase in both arterial perfusion and mean transit time in patients with cirrhosis (Fig. 2) [35, 36]. Perfusion changes were also observed at intermediate stages of liver fibrosis [35, 37]. In cirrhosis, changes were more marked, and we showed that perfusion alteration were correlated with the severity of portal hypertension and the degree of liver dysfunction [35]. Although these results need be confirmed in larger studies, they suggest that DCE-MR imaging may be useful in assessing the severity of cirrhosis.

Perfusion imaging with hepatobiliary contrast agents

The use of a hepatobiliary contrast agent (for instance gadoxetic acid (Primovist; Bayer, Berlin, Germany) enables quantification of both the liver perfusion and the hepatocyte transport function [12, 38]. This is due to the partial uptake of hepatobiliary contrast agents within hepatocytes via the organic anion transporting polypeptides OATP1 B1/B3, followed by biliary excretion through the multidrug resistance protein MRP2 transporters. Sinusoidal backflow also

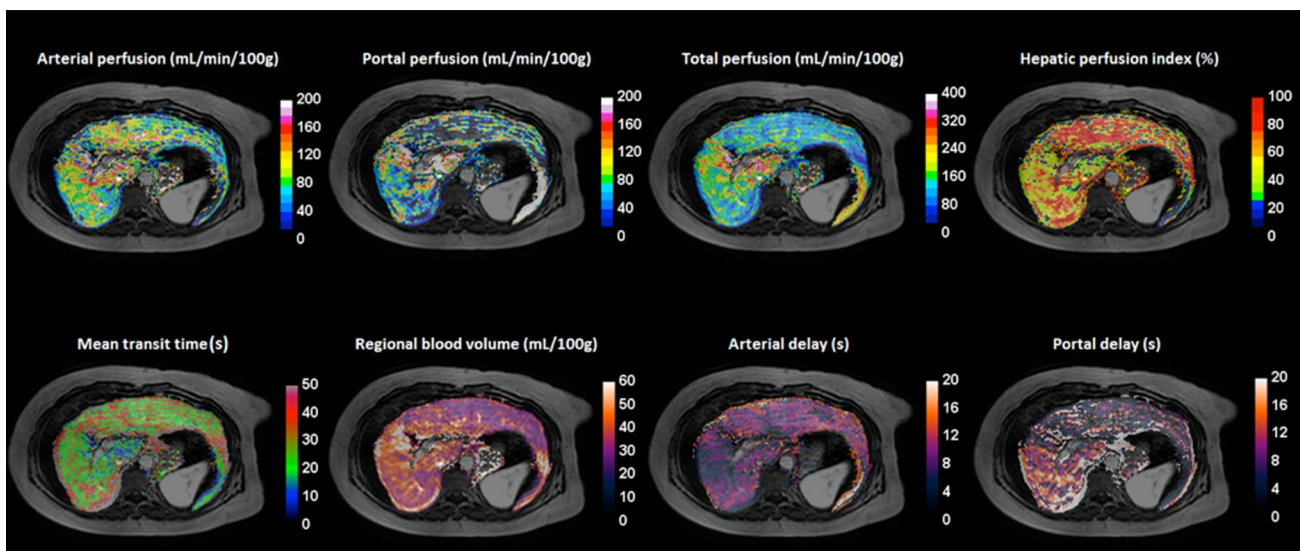


Fig. 2 Example of perfusion parametric maps (arterial, portal and total perfusion, hepatic perfusion index, mean transit time, and regional blood volume) obtained from a patient with cirrhosis. These maps were computed from images acquired with a 4D keyhole acquisition with 1.7 s temporal resolution. Gd-DOTA was used as a tracer. Perfusion parameters were extracted using a non-linear least square fit on a dual-input one-compartment model including delays (arterial and portal). These maps well illustrate the adaptive response in the liver aiming to counterbalance the portal perfusion drop by increasing

arterial perfusion in order to keep the total perfusion. This explains the significant rise in the hepatic perfusion index. Mean transit time increased illustrating the restriction of the low molecular weight tracer molecules in the Disse due to collagen deposition in liver cirrhosis. Mean perfusion parameters values were Arterial, portal, and total perfusion of 72, 54, and 126 mL min⁻¹ 100 g⁻¹, respectively; hepatic perfusion index: 57.1%; mean transit time: 27.2 s; and regional blood volume: 57.1 mL 100 g⁻¹

occurs through MRP3 and the bidirectional OATP1B1/B3 transporters [39].

In chronic liver diseases, expression and function of the hepatocyte transporters change leading to changes of gadoxetic acid enhancement during the hepatobiliary phase. The transporter changes consist mainly in decreased OATP1 B1/B3 and MRP2 expression, increased MRP3 expression, and MRP2 internalization. As we showed in animal models of chronic liver disease, these organic anion transporter changes cause a decrease in liver signal intensity at static gadoxetic acid-enhanced MRI during the hepatobiliary phase, as well as a decrease of the pharmacokinetic rate constants (hepatocyte influx, efflux, and backflux rates) during dynamic MR (Figs. 3, 4, and 5) [40, 41].

Static and dynamic gadoxetic acid-enhanced MRI has been proposed to assess the severity of liver fibrosis, NASH and to evaluate liver function in chronic liver disease [42–44]. We developed a complete dual-input three-compartmental model of liver perfusion and hepatocyte transport function during dynamic gadoxetic acid-enhanced MRI and observed that changes in the hepatocyte transfer rates were earlier markers of liver fibrosis than perfusion parameter changes [7]. Although this dynamic MRI method has the potential to improve the assessment of chronic liver disease relative to the use of a static hepatic enhancement ratio during the hepatobiliary phase, the difficulty of dynamic MRI acquisition up to 40 min after contrast material injection and the pharmacokinetic model complexity may limit its clinical use. Methods that are based on sparse data acquisition may prove to be useful in this context [45]. Besides dynamic imaging, texture analysis and deep learning with

convolutional neural networks might also be promising methods to improve the diagnostic performance of gadoxetic acid-enhanced MRI, but this should be studied further [46, 47].

Finally, as the hepatocyte anion transporters that carry the hepatobiliary contrast agents during their hepatic transport are also used by various drugs, dynamic hepatobiliary-enhanced used imaging may be used in vitro and in vivo to assess transporter inhibition and drug-induced liver injury [48, 49].

Alternative perfusion methods to assess chronic liver disease

Another approach to evaluate liver perfusion is the IVIM model of diffusion MR imaging, as mentioned above. We observed that rats with liver fibrosis had reduced in vivo ADC (apparent diffusion coefficient) values compared to controls, although this difference disappeared ex vivo, underlining the role of decreased perfusion in ADC decrease related to liver fibrosis [16]. A human study published by Luciani et al. confirmed the ADC decrease in patients with liver cirrhosis compared to controls. Authors also showed that the restriction in diffusion was mostly caused by changes in microperfusion and to a lesser extent by reduction in actual diffusion [50]. These results were further confirmed by Yoon et al in patients with chronic liver disease [51], and by Chow et al. and Zhang et al. in rodents [52, 53].

More recently, several teams have investigated the IVIM model for the assessment of non-alcoholic fatty liver disease (NAFLD) with conflicting results. A study by Lee et al. did not

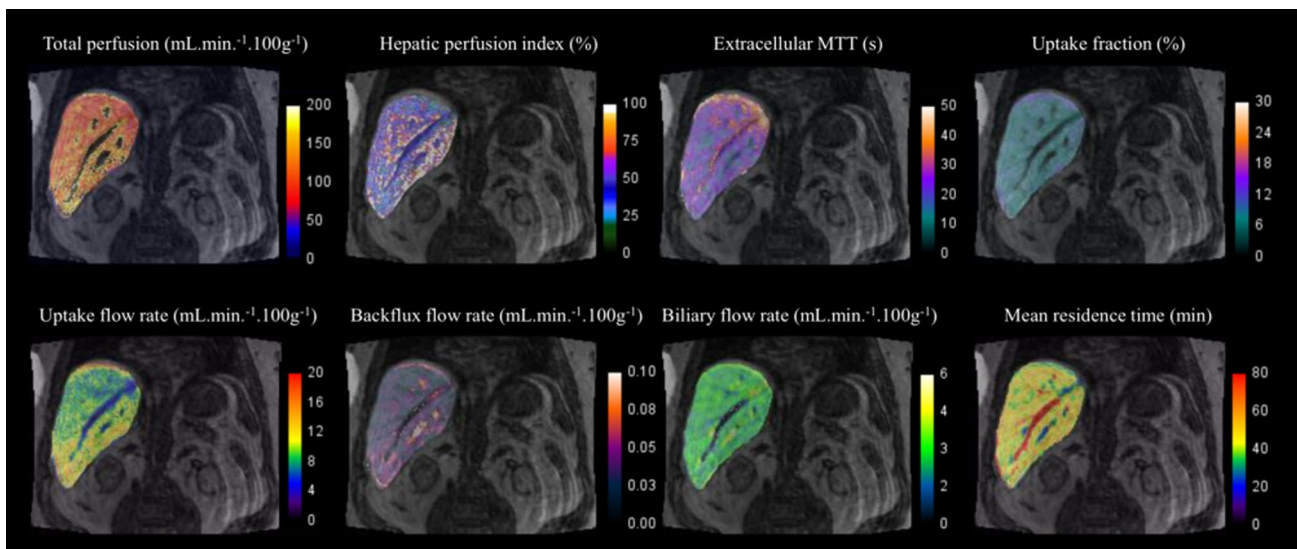


Fig. 3 Parametric maps of liver perfusion and hepatocyte transport at gadoxetic acid-enhanced MRI. Total liver perfusion, hepatic perfusion index (arterial fraction), extracellular mean transit time (MTT),

hepatocyte uptake fraction, hepatocyte uptake rate, hepatocyte backflux, biliary efflux, and hepatic mean residence time can be assessed using a dual-input tri-compartmental hepatobiliary model

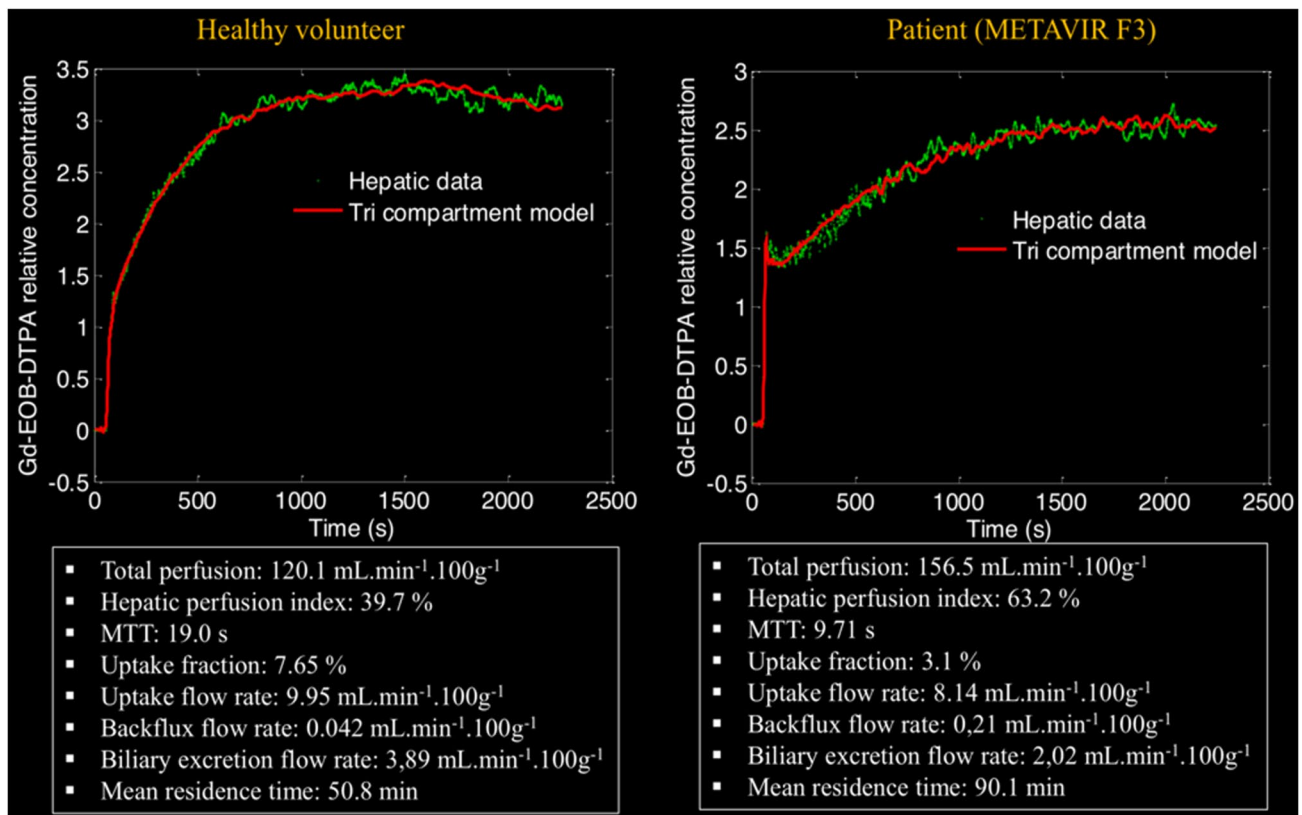


Fig. 4 Hepatic signal intensity enhancement curves after intravenous injection of gadoxetic acid and fitted with dual-input tri-compartmental model in healthy volunteer (left) and patient with advanced liver fibrosis (F3; right). In patient with advanced fibrosis, both perfusion

and hepatocyte transport parameters are changed relative to those in a healthy volunteer. Parameter changes in liver fibrosis include hepatic perfusion index and sinusoidal backflux increase, as well as hepatocyte influx and biliary efflux decrease

report any significant correlation between the IVIM-derived perfusion parameters and the hepatic fat fraction [54], while Guiu et al. [55] found decreased parenchymal perfusion in patients with steatosis. In a rabbit model, Joo et al. showed the perfusion fraction to be significantly lower in animals with NAFLD than in controls with a progressive perfusion decrease as the severity of NAFLD increased [56]. IVIM parameters are probably affected by liver steatosis, but further studies are needed to confirm these results.

Finally, liver perfusion assessment without contrast material injection can also be performed with arterial spin labeling [57]. With this method, acute changes in liver perfusion after a meal challenge have been observed and differences in the response to the meal challenge between controls and patients with liver cirrhosis have been detected [58]. This method might thus be useful to assess liver hemodynamics after physiological challenges.

Conclusion

Perfusion imaging is currently not part of the routine CT or MRI protocol in patients with chronic liver diseases. This method is mainly performed in clinical and experimental research. Results are encouraging, showing the potential use of perfusion imaging in chronic liver diseases. Perfusion changes can be used to assess the severity of cirrhosis and portal hypertension. Perfusion changes can also be observed at earlier stages of chronic liver disease. With hepatobiliary contrast-enhanced MR imaging, liver perfusion and hepatocyte transport can be assessed separately. Hepatocyte transport changes may be earlier markers of chronic liver disease than perfusion changes. Moreover, since hepatocyte transports are much slower than perfusion, the constraints on MR image acquisition speed are

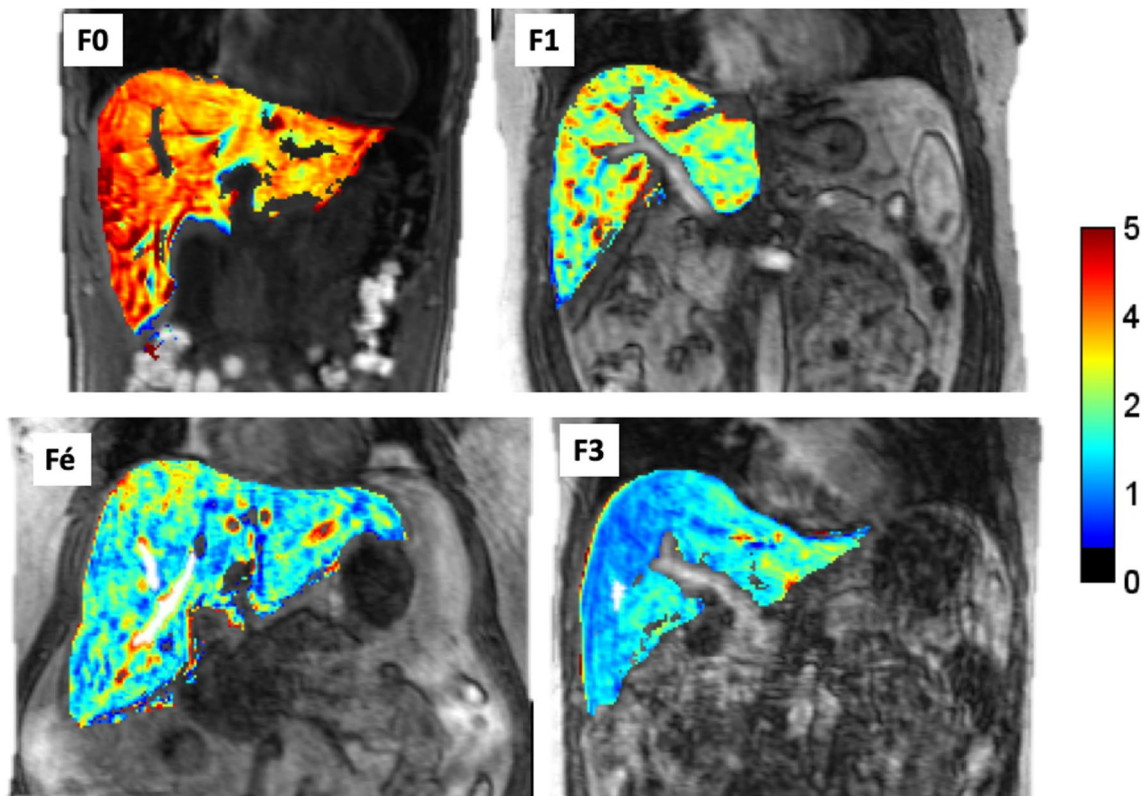


Fig. 5 Parametric maps of biliary efflux at gadoxetic acid-enhanced MRI in patients with progressive fibrosis deposition. Biliary efflux was assessed using a dual-input tri-compartmental hepatobiliary model. Biliary efflux progressively decreases from normal

liver (F0) to advanced fibrosis (F3) ($k_3=3.53 \text{ mL min}^{-1} \cdot 100 \text{ g}^{-1}$, $k_3=2.67 \text{ mL min}^{-1} \cdot 100 \text{ g}^{-1}$, $k_3=2.23 \text{ mL min}^{-1} \cdot 100 \text{ g}^{-1}$, $k_3=1.64 \text{ mL min}^{-1} \cdot 100 \text{ g}^{-1}$ in F0, F1, F2, and F3, respectively)

much lower when assessing hepatobiliary transport than perfusion. This may facilitate the more widespread use of hepatobiliary contrast-enhanced MRI in the assessment of chronic liver disease.

References

- Friedman SL (2003) Liver fibrosis – from bench to bedside. *J Hepatol* 38 Suppl 1:S38-53
- Tacke F (2017) Targeting hepatic macrophages to treat liver diseases. *J Hepatol* 66 (6):1300-1312. <https://doi.org/10.1016/j.jhep.2017.02.026>
- Itai Y, Matsui O (1997) Blood flow and liver imaging. *Radiology* 202 (2):306-314. <https://doi.org/10.1148/radiology.202.2.9015047>
- Pandharipande PV, Krinsky GA, Rusinek H, Lee VS (2005) Perfusion imaging of the liver: current challenges and future goals. *Radiology* 234 (3):661-673. <https://doi.org/10.1148/radiol.2343031362>
- Beck GM, De Becker J, Jones AC, von Falkenhausen M, Willinek WA, Gieseke J (2008) Contrast-enhanced timing robust acquisition order with a preparation of the longitudinal signal component (CENTRA plus) for 3D contrast-enhanced abdominal imaging. *J Magn Reson Imaging* 27 (6):1461-1467. <https://doi.org/10.1002/jmri.21393>
- Chandarana H, Block TK, Rosenkrantz AB, Lim RP, Kim D, Mossa DJ, Babb JS, Kiefer B, Lee VS (2011) Free-breathing radial 3D fat-suppressed T1-weighted gradient echo sequence: a viable alternative for contrast-enhanced liver imaging in patients unable to suspend respiration. *Invest Radiol* 46 (10):648-653. <https://doi.org/10.1097/rli.0b013e31821eea45>
- Leporq B, Daire JL, Pastor CM, Deltenre P, Sempoux C, Schmidt S, Van Beers BE (2018) Quantification of hepatic perfusion and hepatocyte function with dynamic gadoxetic acid-enhanced MRI in patients with chronic liver disease. *Clin Sci (Lond)* 132 (7):813-824. <https://doi.org/10.1042/cs20171131>
- Saranathan M, Rettmann DW, Hargreaves BA, Clarke SE, Vasanawala SS (2012) Differential Subsampling with Cartesian Ordering (DISCO): a high spatio-temporal resolution Dixon imaging sequence for multiphase contrast enhanced abdominal imaging. *J Magn Reson Imaging* 35 (6):1484-1492. <https://doi.org/10.1002/jmri.23602>
- Hedderich DM, Weiss K, Spiro JE, Giese D, Beck GM, Maintz D, Persigehl T (2018) Clinical Evaluation of Free-Breathing Contrast-Enhanced T1w MRI of the Liver using Pseudo Golden Angle Radial k-Space Sampling. *Rofo* 190 (7):601-609. <https://doi.org/10.1055/s-0044-101263>
- Materne R, Smith AM, Peeters F, Dehoux JP, Keyeux A, Horsmans Y, Van Beers BE (2002) Assessment of hepatic perfusion parameters with dynamic MRI. *Magn Reson Med* 47 (1):135-142
- Leporq B, Dumortier J, Pilleul F, Beuf O (2012) 3D-liver perfusion MRI with the MS-325 blood pool agent: a noninvasive

- protocol to assess liver fibrosis. *J Magn Reson Imaging* 35 (6):1380-1387. <https://doi.org/10.1002/jmri.23594>
12. Sourbron S, Sommer WH, Reiser MF, Zech CJ (2012) Combined quantification of liver perfusion and function with dynamic gadoteric acid-enhanced MR imaging. *Radiology* 263 (3):874-883. <https://doi.org/10.1148/radiol.12110337>
 13. Le Bihan D, Breton E, Lallemand D, Grenier P, Cabanis E, Laval-Jeantet M (1986) MR imaging of intravoxel incoherent motions: application to diffusion and perfusion in neurologic disorders. *Radiology* 161 (2):401-407. <https://doi.org/10.1148/radiology.161.2.3763909>
 14. Roberts C, Issa B, Stone A, Jackson A, Waterton JC, Parker GJ (2006) Comparative study into the robustness of compartmental modeling and model-free analysis in DCE-MRI studies. *J Magn Reson Imaging* 23 (4):554-563. <https://doi.org/10.1002/jmri.20529>
 15. Thng CH, Koh TS, Collins DJ, Koh DM (2010) Perfusion magnetic resonance imaging of the liver. *World J Gastroenterol* 16 (13):1598-1609
 16. Annet L, Peeters F, Abarca-Quinones J, Leclercq I, Moulin P, Van Beers BE (2007) Assessment of diffusion-weighted MR imaging in liver fibrosis. *J Magn Reson Imaging* 25 (1):122-128. <https://doi.org/10.1002/jmri.20771>
 17. Tofts PS, Brix G, Buckley DL, Evelhoch JL, Henderson E, Knopp MV, Larsson HB, Lee TY, Mayr NA, Parker GJ, Port RE, Taylor J, Weisskoff RM (1999) Estimating kinetic parameters from dynamic contrast-enhanced T(1)-weighted MRI of a diffusable tracer: standardized quantities and symbols. *J Magn Reson Imaging* 10 (3):223-232
 18. Langen KM, Jones DT (2001) Organ motion and its management. *Int J Radiat Oncol Biol Phys* 50 (1):265-278
 19. Heacock L, Gao Y, Heller SL, Melsaether AN, Babb JS, Block TK, Otazo R, Kim SG, Moy L (2017) Comparison of conventional DCE-MRI and a novel golden-angle radial multicoil compressed sensing method for the evaluation of breast lesion conspicuity. *J Magn Reson Imaging* 45 (6):1746-1752. <https://doi.org/10.1002/jmri.25530>
 20. Weiss J, Ruff C, Grosse U, Grozinger G, Horger M, Nikolaou K, Gatidis S (2019) Assessment of Hepatic Perfusion Using GRASP MRI: Bringing Liver MRI on a New Level. *Invest Radiol*. <https://doi.org/10.1097/rli.0000000000000586>
 21. Chandarana H, Feng L, Ream J, Wang A, Babb JS, Block KT, Sodickson DK, Otazo R (2015) Respiratory Motion-Resolved Compressed Sensing Reconstruction of Free-Breathing Radial Acquisition for Dynamic Liver Magnetic Resonance Imaging. *Invest Radiol* 50 (11):749-756. <https://doi.org/10.1097/rli.0000000000000179>
 22. Feng L, Grimm R, Block KT, Chandarana H, Kim S, Xu J, Axel L, Sodickson DK, Otazo R (2014) Golden-angle radial sparse parallel MRI: combination of compressed sensing, parallel imaging, and golden-angle radial sampling for fast and flexible dynamic volumetric MRI. *Magn Reson Med* 72 (3):707-717. <https://doi.org/10.1002/mrm.24980>
 23. Jajamovich GH, Dyvorne H, Donnerhack C, Taouli B (2014) Quantitative liver MRI combining phase contrast imaging, elastography, and DWI: assessment of reproducibility and post-prandial effect at 3.0 T. *PLoS One* 9 (5):e97355. <https://doi.org/10.1371/journal.pone.0097355>
 24. Goh V, Halligan S, Bartram CI (2007) Quantitative tumor perfusion assessment with multidetector CT: are measurements from two commercial software packages interchangeable? *Radiology* 242 (3):777-782. <https://doi.org/10.1148/radiol.2423060279>
 25. Heye T, Davenport MS, Horvath JJ, Feuerlein S, Breault SR, Bashir MR, Merkle EM, Boll DT (2013) Reproducibility of dynamic contrast-enhanced MR imaging. Part I. Perfusion characteristics in the female pelvis by using multiple computer-aided diagnosis perfusion analysis solutions. *Radiology* 266 (3):801-811. <https://doi.org/10.1148/radiol.12120278>
 26. Heye T, Merkle EM, Reiner CS, Davenport MS, Horvath JJ, Feuerlein S, Breault SR, Gall P, Bashir MR, Dale BM, Kiraly AP, Boll DT (2013) Reproducibility of dynamic contrast-enhanced MR imaging. Part II. Comparison of intra- and interobserver variability with manual region of interest placement versus semiautomatic lesion segmentation and histogram analysis. *Radiology* 266 (3):812-821. <https://doi.org/10.1148/radiol.12120255>
 27. Leach MO, Morgan B, Tofts PS, Buckley DL, Huang W, Horsfield MA, Chenevert TL, Collins DJ, Jackson A, Lomas D, Whitcher B, Clarke L, Plummer R, Judson I, Jones R, Alonzi R, Brunner T, Koh DM, Murphy P, Waterton JC, Parker G, Graves MJ, Scheenen TW, Redpath TW, Orton M, Karczmar G, Huisman H, Barentsz J, Padhani A, Experimental Cancer Medicine Centres Imaging Network Steering C (2012) Imaging vascular function for early stage clinical trials using dynamic contrast-enhanced magnetic resonance imaging. *Eur Radiol* 22 (7):1451-1464. <https://doi.org/10.1007/s00330-012-2446-x>
 28. . https://qibawiki.rsna.org/images/1/12/DCE-MRI_Quantification_Profile_v1.0.pdf. Accessed July 12 2019
 29. Miles KA, Hayball MP, Dixon AK (1993) Functional images of hepatic perfusion obtained with dynamic CT. *Radiology* 188 (2):405-411. <https://doi.org/10.1148/radiology.188.2.8327686>
 30. Blomley MJ, Coulden R, Dawson P, Kormano M, Donlan P, Bufkin C, Lipton MJ (1995) Liver perfusion studied with ultrafast CT. *J Comput Assist Tomogr* 19 (3):424-433
 31. Van Beers BE, Leconte I, Materne R, Smith AM, Jamart J, Horsmans Y (2001) Hepatic perfusion parameters in chronic liver disease: dynamic CT measurements correlated with disease severity. *AJR Am J Roentgenol* 176 (3):667-673. <https://doi.org/10.2214/ajr.176.3.1760667>
 32. Ronot M, Asselah T, Paradis V, Michoux N, Dorvillius M, Baron G, Marcellin P, Van Beers BE, Vilgrain V (2010) Liver fibrosis in chronic hepatitis C virus infection: differentiating minimal from intermediate fibrosis with perfusion CT. *Radiology* 256 (1):135-142. <https://doi.org/10.1148/radiol.10091295>
 33. Van Beers BE, Materne R, Annet L, Hermoye L, Sempoux C, Peeters F, Smith AM, Jamart J, Horsmans Y (2003) Capillarization of the sinusoids in liver fibrosis: noninvasive assessment with contrast-enhanced MRI in the rabbit. *Magn Reson Med* 49 (4):692-699. <https://doi.org/10.1002/mrm.10420>
 34. Zhou L, Chen TW, Zhang XM, Yang Z, Tang HJ, Deng D, Zeng NL, Wang LY, Chen XL, Li H, Li CP, Li L, Xie XY, Hu J (2013) Liver dynamic contrast-enhanced MRI for staging liver fibrosis in a piglet model. *J Magn Reson Imaging*. <https://doi.org/10.1002/jmri.24248>
 35. Annet L, Materne R, Danse E, Jamart J, Horsmans Y, Van Beers BE (2003) Hepatic flow parameters measured with MR imaging and Doppler US: correlations with degree of cirrhosis and portal hypertension. *Radiology* 229 (2):409-414. <https://doi.org/10.1148/radiol.2292021128>
 36. Baxter S, Wang ZJ, Joe BN, Qayyum A, Taouli B, Yeh BM (2009) Timing bolus dynamic contrast-enhanced (DCE) MRI assessment of hepatic perfusion: Initial experience. *J Magn Reson Imaging* 29 (6):1317-1322. <https://doi.org/10.1002/jmri.21795>
 37. Hagiwara M, Rusinek H, Lee VS, Losada M, Bannan MA, Krinsky GA, Taouli B (2008) Advanced liver fibrosis: diagnosis with 3D whole-liver perfusion MR imaging—initial experience. *Radiology* 246 (3):926-934. <https://doi.org/10.1148/radiol.2463070077>
 38. Van Beers BE, Garteiser P, Leporq B, Rautou PE, Valla D (2017) Quantitative Imaging in Diffuse Liver Diseases. *Semin Liver Dis* 37 (3):243-258. <https://doi.org/10.1055/s-0037-1603651>
 39. Van Beers BE, Pastor CM, Hussain HK (2012) Primovist, Eovist: what to expect? *J Hepatol* 57 (2):421-429. <https://doi.org/10.1016/j.jhep.2012.01.031>

40. Giraudeau C, Leporq B, Doblaz S, Lagadec M, Pastor CM, Daire JL, Van Beers BE (2017) Gadoxetate-enhanced MR imaging and compartmental modelling to assess hepatocyte bidirectional transport function in rats with advanced liver fibrosis. *Eur Radiol* 27 (5):1804–1811. <https://doi.org/10.1007/s00330-016-4536-7>
41. Lagadec M, Doblaz S, Giraudeau C, Ronot M, Lambert SA, Fasseu M, Paradis V, Moreau R, Pastor CM, Vilgrain V, Daire JL, Van Beers BE (2015) Advanced fibrosis: Correlation between pharmacokinetic parameters at dynamic gadoxetate-enhanced MR imaging and hepatocyte organic anion transporter expression in rat liver. *Radiology* 274 (2):379–386. <https://doi.org/10.1148/radiol.114140313>
42. Ba-Ssalamah A, Bastati N, Wibmer A, Fragner R, Hodge JC, Trauner M, Herold CJ, Bashir MR, Van Beers BE (2017) Hepatic gadoxetic acid uptake as a measure of diffuse liver disease: Where are we? *J Magn Reson Imaging* 45 (3):646–659. <https://doi.org/10.1002/jmri.25518>
43. Feier D, Balassy C, Bastati N, Stift J, Badaea R, Ba-Ssalamah A (2013) Liver fibrosis: histopathologic and biochemical influences on diagnostic efficacy of hepatobiliary contrast-enhanced MR imaging in staging. *Radiology* 269 (2):460–468. <https://doi.org/10.1148/radiol.13122482>
44. Yoon JH, Lee JM, Kang HJ, Ahn SJ, Yang H, Kim E, Okuaki T, Han JK (2019) Quantitative Assessment of Liver Function by Using Gadoxetic Acid-enhanced MRI: Hepatocyte Uptake Ratio. *Radiology* 290 (1):125–133. <https://doi.org/10.1148/radiol.2018180753>
45. Noren B, Forsgren MF, Dahlqvist Leinhard O, Dahlstrom N, Kihlberg J, Romu T, Kechagias S, Almer S, Smedby O, Lundberg P (2013) Separation of advanced from mild hepatic fibrosis by quantification of the hepatobiliary uptake of Gd-EOB-DTPA. *Eur Radiol* 23 (1):174–181. <https://doi.org/10.1007/s00330-012-2583-2>
46. Kim H, Park SH, Kim EK, Kim MJ, Park YN, Park HJ, Choi JY (2014) Histogram analysis of gadoxetic acid-enhanced MRI for quantitative hepatic fibrosis measurement. *PLoS One* 9 (12):e114224. <https://doi.org/10.1371/journal.pone.0114224>
47. Yasaka K, Akai H, Kunimatsu A, Abe O, Kiryu S (2018) Liver Fibrosis: Deep Convolutional Neural Network for Staging by Using Gadoxetic Acid-enhanced Hepatobiliary Phase MR Images. *Radiology* 287 (1):146–155. <https://doi.org/10.1148/radiol.2017171928>
48. Ulloa JL, Stahl S, Yates J, Woodhouse N, Kenna JG, Jones HB, Waterton JC, Hockings PD (2013) Assessment of gadoxetate DCE-MRI as a biomarker of hepatobiliary transporter inhibition. *NMR Biomed* 26 (10):1258–1270. <https://doi.org/10.1002/nbm.2946>
49. Bonnaventure P, Cusin F, Pastor CM (2019) Hepatocyte Concentrations of Imaging Compounds Associated with Transporter Inhibition: Evidence in Perfused Rat Livers. *Drug Metab Dispos* 47 (4):412–418. <https://doi.org/10.1124/dmd.118.084624>
50. Luciani A, Vignaud A, Cavet M, Nhieu JT, Mallat A, Ruel L, Laurent A, Deux JF, Brugieres P, Rahmouni A (2008) Liver cirrhosis: intravoxel incoherent motion MR imaging—pilot study. *Radiology* 249 (3):891–899. <https://doi.org/10.1148/radiol.2493080080>
51. Yoon JH, Lee JM, Baek JH, Shin CI, Kiefer B, Han JK, Choi BI (2014) Evaluation of hepatic fibrosis using intravoxel incoherent motion in diffusion-weighted liver MRI. *J Comput Assist Tomogr* 38 (1):110–116. <https://doi.org/10.1097/rct.0b013e3182a589be>
52. Chow AM, Gao DS, Fan SJ, Qiao Z, Lee FY, Yang J, Man K, Wu EX (2012) Liver fibrosis: an intravoxel incoherent motion (IVIM) study. *J Magn Reson Imaging* 36 (1):159–167. <https://doi.org/10.1002/jmri.23607>
53. Zhang Y, Jin N, Deng J, Guo Y, White SB, Yang GY, Omary RA, Larson AC (2013) Intra-voxel incoherent motion MRI in rodent model of diethylnitrosamine-induced liver fibrosis. *Magn Reson Imaging* 31 (6):1017–1021. <https://doi.org/10.1016/j.mri.2013.03.007>
54. Lee JT, Liao J, Murphy P, Schroeder ME, Sirlin CB, Bydder M (2012) Cross-sectional investigation of correlation between hepatic steatosis and IVIM perfusion on MR imaging. *Magn Reson Imaging* 30 (4):572–578. <https://doi.org/10.1016/j.mri.2011.12.013>
55. Guiu B, Petit JM, Capitan V, Aho S, Masson D, Lefevre PH, Favelier S, Loffroy R, Verges B, Hillon P, Krause D, Cercueil JP (2012) Intravoxel incoherent motion diffusion-weighted imaging in nonalcoholic fatty liver disease: a 3.0-T MR study. *Radiology* 265 (1):96–103. <https://doi.org/10.1148/radiol.12112478>
56. Joo I, Lee JM, Yoon JH, Jang JJ, Han JK, Choi BI (2014) Nonalcoholic fatty liver disease: intravoxel incoherent motion diffusion-weighted MR imaging—an experimental study in a rabbit model. *Radiology* 270 (1):131–140. <https://doi.org/10.1148/radiol.13122506>
57. Martirosian P, Pohmann R, Schraml C, Schwartz M, Kuestner T, Schwenzer NF, Scheffler K, Nikolaou K, Schick F (2019) Spatial-temporal perfusion patterns of the human liver assessed by pseudo-continuous arterial spin labeling MRI. *Z Med Phys* 29 (2):173–183. <https://doi.org/10.1016/j.zemedi.2018.08.004>
58. Cox EF, Palaniyappan N, Aithal GP, Guha IN, Francis ST (2019) Using MRI to study the alterations in liver blood flow, perfusion, and oxygenation in response to physiological stress challenges: Meal, hyperoxia, and hypercapnia. *J Magn Reson Imaging* 49 (6):1577–1586. <https://doi.org/10.1002/jmri.26341>

Publisher's Note Springer Nature remains neutral with regard to jurisdictional claims in published maps and institutional affiliations.